Mutations in the *SC4MOL* gene encoding a novel methyl sterol oxidase cause autosomal recessive psoriasisiform dermatitis, microcephaly and developmental delay

Miao He [1,2], Lisa E. Kratz [4], Joshua J. Michel[1,2], Abbe N. Vallejo[1,2,3], Laura Ferris [2]., Richard I. Kelley [4], Jacqualine J. Hoover[1], K. Michael Gibson [1,2], Jerry Vockley[1,2].
Children's Hospital of Pittsburgh[1], Departments of Pediatrics[2] and Immunology[3], University of Pittsburgh School of Medicine, Pittsburgh, PA; The Kennedy Krieger Institute[4], Baltimore, MD.

Summary

Disorders of cholesterol biosynthesis have clinical manifestations involving skeleton, eyes, neurologic development, and skin[1]. We describe a patient with congenital cataracts, developmental delay, microcephaly, and low serum cholesterol who developed severe psoriasiform dermatitis and arthralgias beginning at age 3. Her brain MRI indicated minor gliosis. Quantitative sterol analysis of patient plasma and skin showed marked elevation of 4α-methyl- and 4, 4'-dimethylsterols, indicating a deficiency in the first step of sterol C4 demethylation in cholesterol biosynthesis. Molecular studies showed mutations in *SC4MOL*, a gene predicted to encode a sterol C4 methyl oxidase. Thus, our patient has a previously undescribed inborn error of cholesterol biosynthesis. Cellular studies with patient-derived fibroblasts showed higher mitotic rate than control cells in cholesterol-depleted medium, in which *de novo* cholesterol biosynthesis was increased with the accumulation of methylsterol. Immunologic analyses showed dysregulation of immune-related receptors in the patient and her father. Inhibition of sterol C4 methyl oxidase in human transformed lymphoblasts or in fresh leukocytes induced activation of cell cycle, and immune receptor dysregulation . These findings suggest that methylsterols influence mitotic capacity and immune function. *SC4MOL* is situated within the psoriasis susceptibility locus *PSORS9*[2], and is likely a genetic risk factor for common psoriasis.

The patient was seen in our clinic at the age of 13. She had a severe dermatitis affecting her entire body, sparing the palms (**Fig 1a-c**). Skin biopsy was characteristic of psoriasiform dermatitis (**Fig 1d**). While her skin briefly improved with cyclosporine A treatment, she did not respond to other treatments including topical corticosteroids, dovonex, etanercept, phototherapy, and oral isotretinoin. The refractory nature of her skin disease, and mild developmental and growth delay with delayed skeletal maturation, a history of multiple allergies, mild arthritis, and frequent infections, prompted further evaluation. She had markedly elevated levels of serum IgE at 1,486 IU/ml (normal <180) and IgA at 684 IU/ml (normal <218). Her serum lipid profile showed only a persistently low total cholesterol level (**Fig 2c**).

A cholesterol biosynthesis defect was suspected. Analysis of plasma sterols by gas chromatography-mass spectrometry (GC-MS) showed 20- and 500-fold elevation of 4α-monomethyl sterols and 4, 4'-dimethyl sterols, respectively (**Fig 2a**). This pattern of elevation has not been previously associated with a defect in the sterol synthesis pathway, but was consistent with a defect in a methylsterol oxidase.

Therefore, we sequenced the *SC4MOL* gene that was predicted to encode this enzyme. Two variations from the published sequence were identified; 519T>A and 731A>G encoding H173Q and Y244C, respectively, in the sterol C4 methyl oxidase-like protein (**Fig 3a**), herein referred to as sterol methyl oxidase (SMO). The 519T>A mutation was carried by the patient's father, and the 731A>G was carried by the mother. Both amino acids occur within highly conserved metal-binding domains in SMO (**Fig 3b**). In addition, H173Q alters a predicted active site of the second iron-binding motif of the enzyme.

Plasma methylsterol levels were also elevated in the patient's parents (**Fig 2c**). This suggests a subclinical effect for heterozygotes, in keeping with that seen in carriers of a *DHCR14B/LBR* mutation who have altered nuclear morphology in granulocytes (Pelger-Huët anomaly)[3]. *DHCR14B/LBR* encodes C14-sterol reductase, immediately upstream of SMO, which also functions as a nuclear lamin B receptor[4]. Tight regulation of these two enzymes in the pathway underscores extra-sterol functions of 4, 4'-dimethylsterols.

The two most abundant dimethylsterols; 4, 4'-dimethyl-5α-cholesta-8,24-dien-3β-ol (testis-meiosis activating sterol (MAS)), and 4, 4'-dimethyl-5α-cholesta-8, 14, 24-trien-3β-ol (follicular fluid -MAS), substrates for SMO and C14-sterol reductase respectively, are members of the MAS family and are found in high concentration in testis and ovary. The underlying mechanism of their extra-sterol function remains unknown. However since 4, 4'-dimethylsterols are either direct substrates or products of C14 sterol reductase, they could function as signaling sterols for nuclear lamin B receptor. The nuclear lamin B receptor is important for nuclear membrane breakdown during meiosis of germinal cells[5,6] and formation of the mature granulocyte nucleus[7]. Granulocyte/neutrophil-rich pathology is characteristic of psoriasis and psoriatic arthritis[8,9]. Thus the mild elevation of 4, 4'-dimethylsterols seen in the patient's father could be relevant to his history of mild inflammatory joint disease and a paternal family history of early onset inflammatory joint disease (**Supplementary Fig 1** online**).**

Skin cell hyperproliferation causes flaking skin, characteristic of psoriasis. All known genetic disorders that cause increased levels of MASs, including defects in *DHCR14/LBR, NSDHL* and *EBP* (**Fig 2b**)[1,10,11], present with ichythyosiform/psoriasiform dermatitis in humans and mice. However, none of the defects adjacent or distal to MAS demethylation complex, including *CYP51*, *SC5D*, or *DHCR7*, manifest skin lesions [12-14]. Previous studies of germinal cells have demonstrated meiosis-activating function of MAS [15,16], but the effect of MAS on cell cycle regulation and mitosis is unknown.

Therefore, we examined cell proliferation in patient skin fibroblasts (**Fig 4a-c**). The rate of cell division was found to be higher in patient fibroblast than control cells cultured in cholesterol-depleted medium, a condition under which *de novo* cholesterol biosynthesis is stimulated (**Fig 4a**). The S-G2-M to G0-G1 ratio in patient skin fibroblasts was >3-fold higher than control cells (**Fig 4b**). This ratio peaked after 2-3 days growth in the cholesterol-depleted medium, and corresponded with peaks of cellular methylsterols and total protein (**Supplementary Table 1** online).

Growth of patient cells in cholesterol-depleted suggest association between MAS and cell division. To further examine this possibility, transformed human lymphoblasts were cultured in the presence of a SMO inhibitor, 3-amino-1,2,4-triazole (ATZ). Under these conditions, the cells accumulated a profile of methylsterols similar to that of the patient's lymphocytes grown without ATZ (data not shown). Parallel to this, the S-G2-M/G0-G1 ratio increased 3-fold in treated lymphoblasts, while neither simvastatin or fluconazole (an inhibitor of lanosterol 14α demethylase (*CYP51*)) had a significant effect on cell cycle progression (**Fig 4c**). These data indicate alterations in SMO that in turn affects cell cycle activation.

Patients with genetic defects in *NSDHL,* which encodes the enzyme immediately downstream of SMO, occasionally present with symptoms nearly identical to those with defects in *EBP*[1,10,11] and *vice versa*; but they always differ in skin histopathology. Out of newborn period, *NSDHL*-deficient patients have psoriasiform dermatitis whereas *EBP*-deficient patients have ichthyosis, a condition associated with minor skin inflammation. Our patient, and *NSDHL*-deficient patients accumulate 4, 4'-dimethylsterols in their skin, but *EBP*-deficient patients do not. This suggests that dimethylsterols differ from other MAS in contributing to the perturbation of immune function. *SC4MOL* is located on 4q32-34, the known psoriasis susceptibility locus *PSORS9* (4q31-34). Histologically, our patient's dermatitis is identical with that seen in classical psoriasis.

Since both the patient and her father had a significant elevation of dimethylsterols, we examined a comprehensive panel of immunologic parameters as described in the methods and **Supplementary Table 2** online**.** Selected multicolor flow cytometry profiles of granulocytes and T cells are shown in **Figure 4d**, and the geometric mean fluorescence intensity, and percentage of cells for each measurement are shown in **Supplementary Table 3** online.

We found that activated $CD16^+$ granulocytes; identified by $CD25^+CD69^+$ and $CD86^+HLA\text{-}DR^+$ subsets; were increased 30- and 20-fold in the patient and father, respectively, compared with healthy controls (**Fig 4d** and **Supplementary Table 3** online). In addition, there was 30- and 15-fold increased numbers of toll-like receptor (TLR)-$2^+TLR\text{-}4^-$ granulocytes in the patient and father, respectively, compared with healthy controls (**Fig 4d).** Up-regulation of TLR-2, but not TLR-4, is considered typical for patients with psoriasis[17] or psoriatic arthritis[18]. Over-expression of TLR-2 and down-regulation of TLR-4 on granulocytes suggest perturbation of innate immune responses to bacterial infection. Consistent with this observation, expression of granulocyte-specific, CD16b isoform was also markedly down-regulated in both patient and father (**Fig 4e**), suggesting a defect in phagocytic function.

In the lymphocyte compartment, both patient and father had significantly higher proportions of $CD8^{dim}$ T cells that were also $CD28^{null}CD56^+$ (**Fig 4d, Supplementary Table 3**). Down-regulation of CD8 and CD28, and accumulations of $CD28^{null}CD56^+$ T cells are indicative of pervasive immune activation in the setting of chronic inflammatory disease [19].

We then examined whether inhibiting SMO by ATZ affected normal leukocytes. Results showed over 6-fold increase in TLR-2^{+}TLR-4^{-} granulocyte population (**Fig 4f**), and 2-fold decrease in CD8 expression in normal lymphocytes (**Supplementary Table 4** online). These results recapitulated the *in vivo* granulocyte and T cell phenotypes of the patient and father (**Fig 4d**). All these data indicate a link between cholesterol homeostasis and immunity.

Because psoriasis and psoriatic arthritis are known to be driven by the production of certain cytokines, including tumor necrosis factor (TNF)-α and interleukin (IL)-6, the serum cytokine profiles of the patient and father were investigated by multiplex assay (**Supplementary Table 5** online). Consistent with the flow cytometry data, a number of cytokines and chemokines associated with granulocyte and monocyte activation were elevated in the patient, and to a lesser extent in her father. This included granulocyte and monocyte colony stimulation factor, which is known to trigger psoriasiform eruption in humans[20]. The patient also had elevated IL-6 and IL-8 (**Supplementary Table 5** online), cytokines that amplify skin inflammation as has been demonstrated in psoriatic skin and fibroblasts[21].

The classical pro-inflammatory cytokine TNF-α was normal in the patient, consistent with the fact that her dermatitis did not respond to treatment with etanercept. Cultures of patient skin fibroblasts showed constitutive production of IL-6 compared to control fibroblasts regardless of passage number (**Fig 4g**), and were further increased with the addition of recombinant TNF-α, a known inducer of IL-6. To investigate a possible association of the defect in cholesterologenesis and cytokine production, we treated control and patient fibroblasts with simvastatin, which blocks cholesterol biosynthesis upstream of SMO. After 24 hours, IL-6 production by patient fibroblasts was significantly decreased even in the presence of exogenous TNF-α (**Fig 4g**), suggesting that the accumulated sterol intermediates in our patient were stimulating IL-6 production.

In summary, we have identified the first patient deficient in SMO, a novel enzyme in the C4 methylsterol demethylation complex that is encoded by *SC4MOL*. Our data suggest a role for SMO in regulating granulocyte activation, CD8 expression on T cells, cytokine production, and cell proliferation, factors that are critical in the pathogenesis of common psoriasis. We have previously reported elevated methylsterols in skin flakes from patients with common psoriasis[22]. Thus variation in expression or function of SMO may be an important modifying factor in the development of common psoriasis.

Methods

This study was conducted pursuant to an IRB protocols approved by the University of Pittstburgh.

Genomic DNA and cDNA amplification and sequencing. Total RNA and gDNA was extracted from patient fibroblasts for reverse transcription, PCR amplification, and sequencing as described [23]. Six exons of *SC4MOL* were amplified using intronic primers (all primer sequences available upon request).

Sterol analyses. Sterol distribution was measured in cultured skin fibroblasts, transformed lymphocytes, serum, or skin flakes obtained from patients and controls by GC and selected-ion MS as described[11,24].

Flow cytometry on peripheral blood cells
Flow cytometry on cells from patient and controls were carried out and analyzed as described previously [19,21]. In the sterol oxidase inhibition studies, 10 ml of erythrocyte-depleted blood from a healthy 16-year old girl was incubated with 5mM ATZ for 60 hours at 37 degree with 5% $C0_2$, both ATZ treated and untreated total leukocytes were then isolated and stained as described in Supplementary Table 2 online.

Serum cytokine quantification. Cytokine levels were determined by multiplex assay using the Luminex system (Luminex Corporation) as described previously[25,26].

Cell culture, proliferation and ELISA.
Primary dermal fibroblasts were cultured in DMEM supplemented with 10% FBS, 100 U/ml penicillin, 100 mg/ml streptomycin and GlutaMAX (Invitrogen), TNF-α (10ng/ml) and simvstastin (5μM) were added to fibroblasts at 80% confluency, and culture media were collected after 24 hours for measurement of IL-6 using an ELISA kit (BD Bioscience). For cell proliferation assays, primary fibroblasts or EBV-transformed human lymphoblasts were cultured with cholesterol-depleted medium as described[24]; and ATZ (2mM), simvstastin (5μM) or fluconazole (12.5μM) were added to the medium before the cells were subjected to the proliferation assay.

Cell proliferation and cell cycle stage analysis
Skin fibroblasts, or EBV-transformed lymphoblast (2 x 10^7 cells/ml) were labeled with 0.25μM of 5- (and 6-) carboxyfluorescein diacetate succinimidyl ester (CFSE; Molecular Probes) using established procedures[20]. At different days of culture, cells were harvested and stained with 4',6'-diamidino-2-phenylindole (DAPI), and analyzed by multicolor flow cytometry. The number of cell divisions was determined by the number of CFSE fluorescence peaks. The number of cells in G0-G1 and in the S-G2-M phases of the cell cycle was proportional to the amount of linear DAPI fluorescence, G0-G1 cells having half the amount of DAPI staining as the S-G2-M cells.

Figure Legend

Figure 1. *Severe, scaling,and psoriasiform dermatitis in the patient.* **a**. Note mild microcephaly, lusterless fine fair hair, and blepharitis on face. **b** and **c**. The ichythyosiform erythroderma covers all of the patient's body except for the palms and soles. **d**. H&E-stained section of affected skin shows hyperkeratosis, loss of granular layer, psoriasiform hyperplasia, thinning of suprapaillary plate, and neutrophilic epidermal infiltration; these features are characteristic of psoriasis. Photograph is shown per signed informed consent/assent provided by the patient and her family.

Figure 2. *Sterol profiles of patient samples and diagram of the sterol C4 demethylation pathway.* ***a&b***. Gas chromatographic flame ionization profiles of sterol extracts of patient skin (a) and plasma (b). The ordinates are detector response and elution time. The identified compounds are: 1, internal standard (epicoprostanol); 2, cholesterol; 3, lathosterol; 4, phytosterol; 5, campesterol; 6, 4α-methyl-5α-cholest-8(9)-en-3β-ol; 7, 4α-methyl-5α-cholest-7(8)-en-3β-ol; 8, 4, 4'-dimethyl-5α-cholesta-8(9)-en-3β-ol; 9, lanosterol; 10, sitosterol; 11, 4, 4'-dimethyl-5α-cholesta-8(9),24-dien-3β-ol. Both dimethylsterols and monomethylsterols were markedly elevated in patient skin and plasma. Dimethylsterol (peak 8) is most elevated in skin suggesting the preferential accumulation of 4, 4'-dimethylsterols in the patient's skin compared to plasma, which may explain the severe involvement of the patient's skin. The absence of a 4-carboxysterol in the skin excludes a possible defect in *NSDHL*. ***b***, Diagram of the enzymatic pathway for conversion of lanosterol to cholesterol. The saturation of the C-24 double bond may occur at different points in the pathway. The physiological function *TM7SF2* is unclear[27]. **c**. Plasma sterol analysis and plasma total cholesterol levels from controls, the patient before cholesterol supplementation and after 3 months of cholesterol supplementation, and the patient's mother and father. Methylsterols levels are the sum of both dimethylsterols and monomethylsterols. After 3 month of cholesterol supplementation, a 19% reduction in the patient's plasma methylsterol level was seen, together with an increase of her total cholesterol level. After 6 month of cholesterol supplementation, the patient's total cholesterol normalized, however no further reduction of methylsterols was seen (data not shown).

Figure 3. *Mutation analysis of SC4MOL in proband and parental samples, and the alignment of amino acid sequences of SMO among different species*.
a. Two mutations were identified in *SC4MOL* from both gDNA and cDNA extracted from peripheral blood leukocytes, T519>A and A731>G. T519>A was also identified in gDNA from patient's father, and A731>G was identified in her mother. **b**. Alignment of SMO protein sequences across evolution. From yeast to human, *SC4MOL* is highly conserved. Four conserved metal-binding domains were identified and are highlighted with black squares. The conserved metal binding motifs HXXXH/D and HXXHH are marked under the alignment. T519>A changes amino acid H173 to Q, which replaces the histidine at an active site of the second metal binding domain with glutamine; A731>G changes amino acid Y244 to C; Y244 is in the fourth metal binding domain and also is conserved across evolution.

Figure 4. *Fibroblast and immunocyte abnormalities in the patient and her father.* **a,b:** Fibroblasts were labeled with CFSE and DAPI, cultured, and analyzed by flow cytometry. The number of cell divisions was determined by the number of CFSE fluorescence peaks. The number of cells in G0-G1 and in the S-G2-M phases of the cell cycle was analyzed by the amount of linear DAPI fluorescence. **c** Histograms show typical DAPI fluorescence profiles of cells in G0-G1 and G2-S-M phases of the cell cycle in human EBV-transformed lymphoblasts cultured in standard FBS-supplemented media (FBS); or in cholesterol-depleted medium (CD); or in CD supplemented with either simvastatin (ST), 3-amino-1,2,4 triazole (ATZ), or fluconazole (FA). **d,e:** Leukocyte populations were analyzed by multicolor flow cytometry; subsets identified by forward/scatter profiles, with mature granulocytes, monocytes, and lymphocytes falling in gates A, B, and C, respectively. Data shown are cytometric profiles for CD25, CD69, CD86, HLA-DR, TLR-2, and TLR-4 (**d**), and fluorescence histograms of CD16b (**e)** for mature granulocytes/neutrophils. Also shown are the CD4, CD8, profiles of $CD3^{+}$ T cells; and $CD28^{null}$ $CD56^{+}$ in $CD8^{dim}$ T cells (gate D). No significant differences were observed in the monocyte population (data not shown). **f**. Cytometric profiles for TLR-2 and TLR-4 on granulocytes of healthy control with (blue) or without (red) ATZ treatment. Overlay of cytograms show ATZ-induced phenotypic shift towards increased TLR-2 expression. **g;** IL-6 production by dermal fibroblasts from healthy control and patient upon treatment of TNF-α, and TNF-α plus simvastatin, or in media alone**.**

Acknowledgements

We thank Lynne. A. Wolfe for help with obtaining patient tissue samples, and Lorna Cropcho for assistance in establishment of patient cell lines. These studies were supported by Smith-Lemli-Opitz /RSH Foundation Research Grant and by SIMD/Ucyclyed fellowship grant (both to M.H.); and in part by NIH grant R01 AG022379 (A.N.V.) and by Tobacco Formula Funding from Pennsylvania Department of Health (J.V.).

Reference

1. Herman, G.E. Disorders of cholesterol biosynthesis: prototypic metabolic malformation syndromes. *Hum Mol Genet* **12 Spec No 1**, R75-88 (2003).
2. Zhang, X.J. et al. Evidence for a major psoriasis susceptibility locus at 6p21(PSORS1) and a novel candidate region at 4q31 by genome-wide scan in Chinese hans. *J Invest Dermatol* **119**, 1361-6 (2002).
3. Hoffmann, K. et al. Mutations in the gene encoding the lamin B receptor produce an altered nuclear morphology in granulocytes (Pelger-Huet anomaly). *Nat Genet* **31**, 410-4 (2002).
4. Silve, S., Dupuy, P.H., Ferrara, P. & Loison, G. Human lamin B receptor exhibits sterol C14-reductase activity in Saccharomyces cerevisiae. *Biochim Biophys Acta* **1392**, 233-44 (1998).
5. Mylonis, I. et al. Temporal association of protamine 1 with the inner nuclear membrane protein lamin B receptor during spermiogenesis. *J Biol Chem* **279**, 11626-31 (2004).
6. Byskov, A.G., Andersen, C.Y. & Leonardsen, L. Role of meiosis activating sterols, MAS, in induced oocyte maturation. *Mol Cell Endocrinol* **187**, 189-96 (2002).
7. Hoffmann, K., Sperling, K., Olins, A.L. & Olins, D.E. The granulocyte nucleus and lamin B receptor: avoiding the ovoid. *Chromosoma* **116**, 227-35 (2007).
8. Schon, M., Denzer, D., Kubitza, R.C., Ruzicka, T. & Schon, M.P. Critical role of neutrophils for the generation of psoriasiform skin lesions in flaky skin mice. *J Invest Dermatol* **114**, 976-83 (2000).
9. Kanekura, T., Hiraishi, K., Kawahara, K., Maruyama, I. & Kanzaki, T. Granulocyte and monocyte adsorption apheresis (GCAP) for refractory skin diseases caused by activated neutrophils and psoriatic arthritis: evidence that GCAP removes Mac-1-expressing neutrophils. *Ther Apher Dial* **10**, 247-56 (2006).
10. Shultz, L.D. et al. Mutations at the mouse ichthyosis locus are within the lamin B receptor gene: a single gene model for human Pelger-Huet anomaly. *Hum Mol Genet* **12**, 61-9 (2003).
11. Liu, X.Y. et al. The gene mutated in bare patches and striated mice encodes a novel 3beta-hydroxysteroid dehydrogenase. *Nat Genet* **22**, 182-7 (1999).
12. Kelley, R.I. & Herman, G.E. Inborn errors of sterol biosynthesis. *Annu Rev Genomics Hum Genet* **2**, 299-341 (2001).
13. Jira, P.E. et al. Simvastatin. A new therapeutic approach for Smith-Lemli-Opitz syndrome. *J Lipid Res* **41**, 1339-46 (2000).
14. Krakowiak, P.A. et al. Lathosterolosis: an inborn error of human and murine cholesterol synthesis due to lathosterol 5-desaturase deficiency. *Hum Mol Genet* **12**, 1631-41 (2003).
15. Xie, H. et al. Roles of gonadotropins and meiosis-activating sterols in meiotic resumption of cultured follicle-enclosed mouse oocytes. *Mol Cell Endocrinol* **218**, 155-63 (2004).

16. Cukurcam, S. et al. Influence of follicular fluid meiosis-activating sterol on aneuploidy rate and precocious chromatid segregation in aged mouse oocytes. *Hum Reprod* **22**, 815-28 (2007).
17. Begon, E. et al. Expression, subcellular localization and cytokinic modulation of Toll-like receptors (TLRs) in normal human keratinocytes: TLR2 up-regulation in psoriatic skin. *Eur J Dermatol* **17**, 497-506 (2007).
18. Candia, L., Marquez, J., Hernandez, C., Zea, A.H. & Espinoza, L.R. Toll-like receptor-2 expression is upregulated in antigen-presenting cells from patients with psoriatic arthritis: a pathogenic role for innate immunity? *J Rheumatol* **34**, 374-9 (2007).
19. Michel, J.J. et al. CD56-expressing T cells that have features of senescence are expanded in rheumatoid arthritis. *Arthritis Rheum* **56**, 43-57 (2007).
20. Cho, S.G. et al. Psoriasiform eruption triggered by recombinant granulocyte-macrophage colony stimulating factor (rGM-CSF) and exacerbated by granulocyte colony stimulating factor (rG-CSF) in a patient with breast cancer. *J Korean Med Sci* **13**, 685-8 (1998).
21. Debets, R. et al. Expression of cytokines and their receptors by psoriatic fibroblast. I. Altered IL-6 synthesis. *Cytokine* **8**, 70-9 (1996).
22. Grange DK, H.G., Kelley RI, Kratz LE, Kopacz KJ, Siegfried E. Abnormal Laterality Development and Proliferative Epidermal Skin Lesions in X-Linked Disorders of Cholesterol Biosynthesis. *Proc. Greenwood Gen Center* **20**, 105 (2001).
23. He, M. et al. A new genetic disorder in mitochondrial fatty acid beta-oxidation: ACAD9 deficiency. *Am J Hum Genet* **81**, 87-103 (2007).
24. Kelley, R.I. Diagnosis of Smith-Lemli-Opitz syndrome by gas chromatography/mass spectrometry of 7-dehydrocholesterol in plasma, amniotic fluid and cultured skin fibroblasts. *Clin Chim Acta* **236**, 45-58 (1995).
25. de Jager, W., Prakken, B.J., Bijlsma, J.W., Kuis, W. & Rijkers, G.T. Improved multiplex immunoassay performance in human plasma and synovial fluid following removal of interfering heterophilic antibodies. *J Immunol Methods* **300**, 124-35 (2005).
26. Pfleger, C., Schloot, N. & ter Veld, F. Effect of serum content and diluent selection on assay sensitivity and signal intensity in multiplex bead-based immunoassays. *J Immunol Methods* **329**, 214-8 (2008).
27. Wassif, C.A. et al. HEM dysplasia and ichthyosis are likely laminopathies and not due to 3beta-hydroxysterol Delta14-reductase deficiency. *Hum Mol Genet* **16**, 1176-87 (2007).

Figure 1, He, et al., 2008

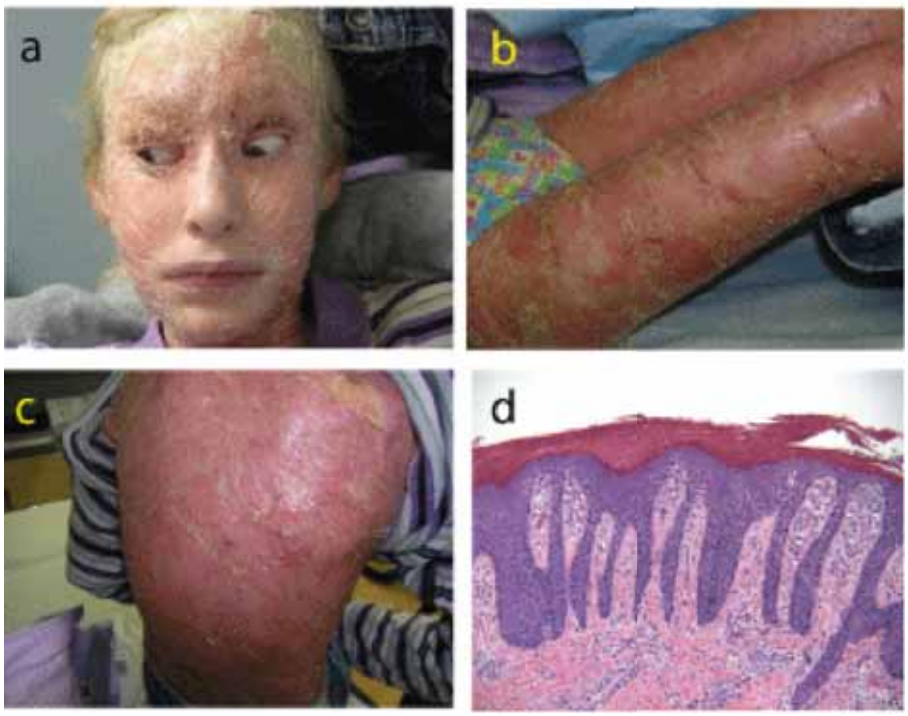

He, et al., 2008

a skin

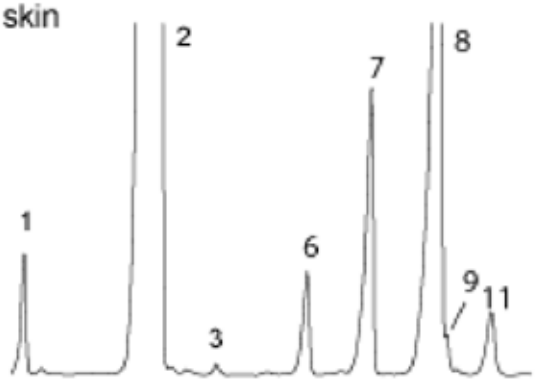

b plasma

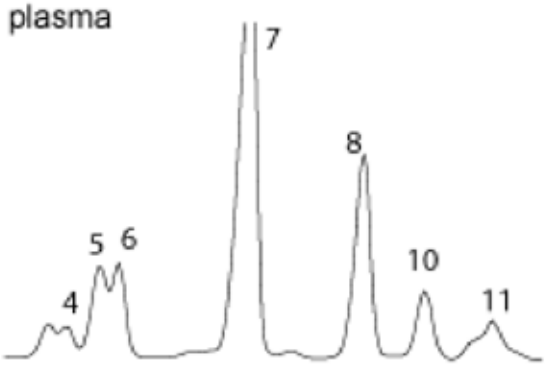

c

	Methyl sterols (μg/ml)	Total Cholsterol (mg/dl)
Normal	3.0 ± 2	140-176
Patient	43	85
Patient + Cholesterol	31	124
Mother	6.4	188
Father	18.5	231

d

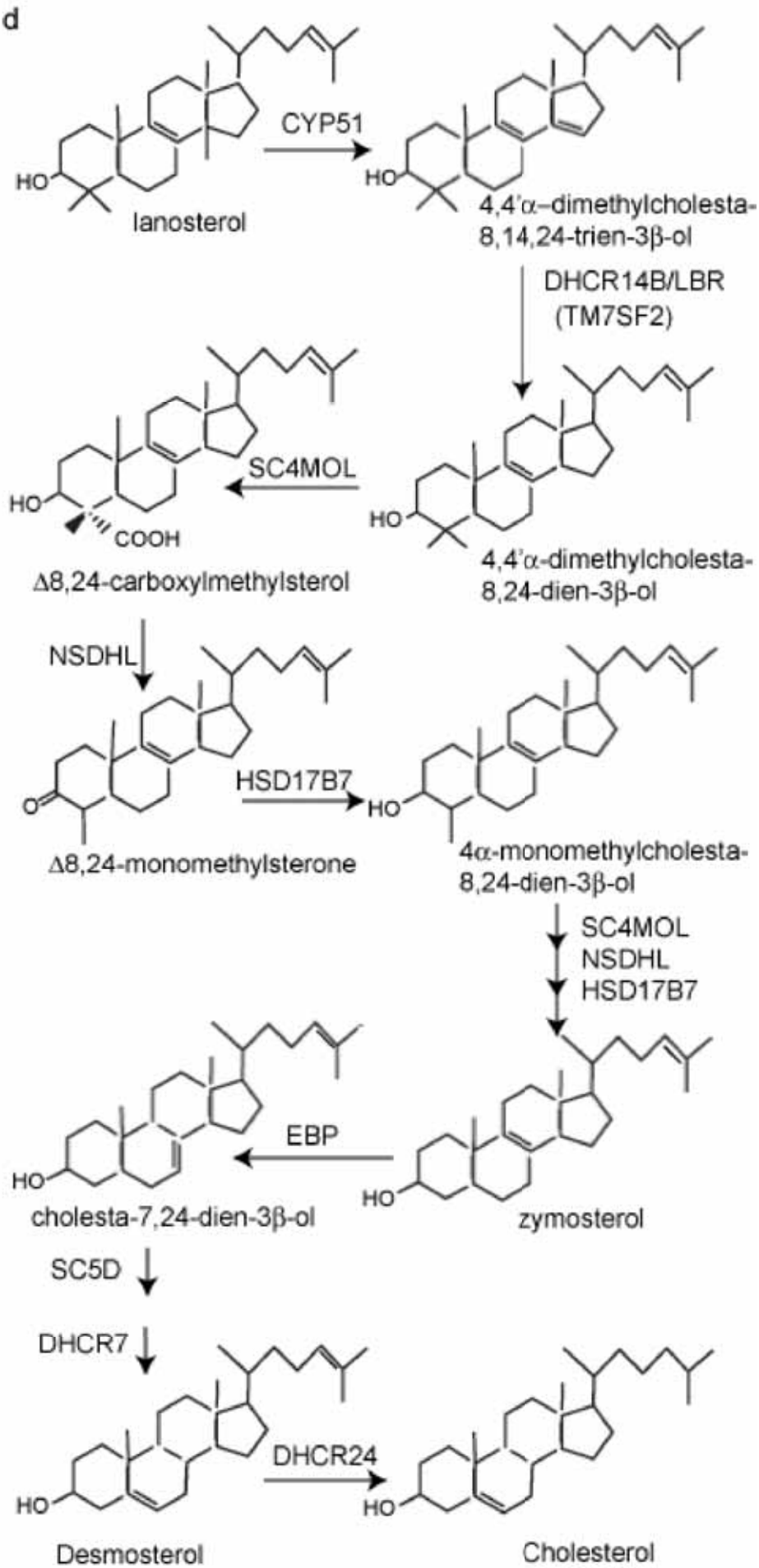

Figure 3, He, et al., 2008

a

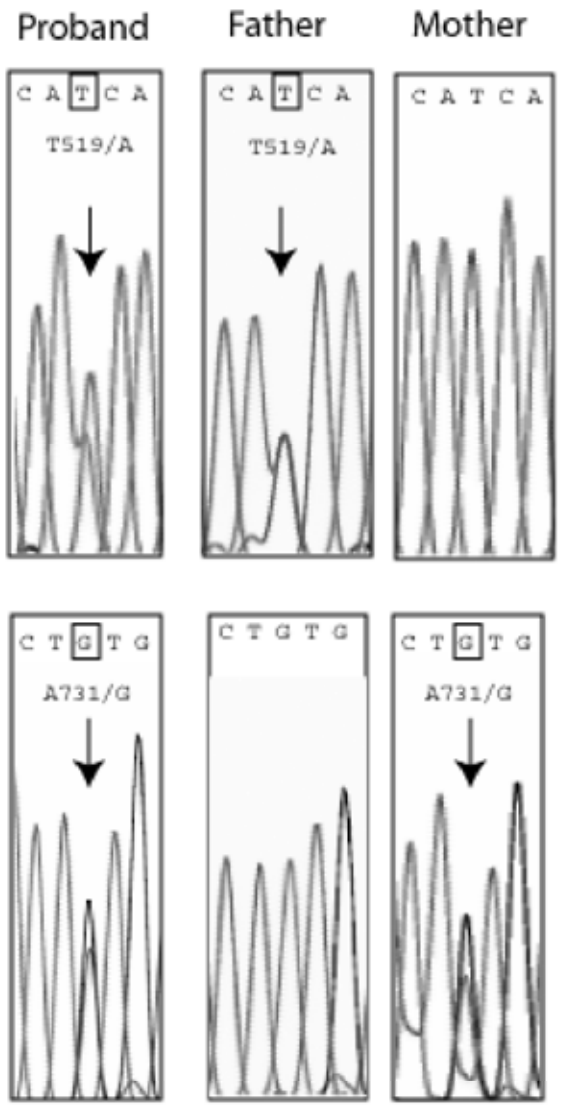

b

```
Human     1   ----------------MATNESVSIP-SSASLAVEYVDSLLP----------ENPLQ   30
Chimp     1   MEMADYSRQKGQFEQKHGGMKQQYSVFRSSQALTGNLPGTQLPRRLRAAGRGGHPSVP   59
Dog       1   ----------------MATNESISIF-SSASLAVEYVDSLLP----------ENPLQ   30
Mouse     1   ----------------MATNKSVGVF-SSASLAVEYVDSLLP----------ENPLQ   30
Rat       1   ----------------MAMNKSVGLP-SSASLAVDYVDSLLP----------ENPLQ   30
Yeast     1   --------------MSAVFNNATLSGLV----QASTYSQTLQN-------VAHYQPQL   27

Human    31   EPFKNAWNYMLNNYTKFQIAT-WGSLIVHEALYFLFCLPGFLFQFI-----------   75
Chimp    60   APSRRDALSRFPASGRSAVPT-IGWPCRSHYPHSIRGANGNDRQELDGPPGPPGSTPQ  115
Dog      31   EPFKNAWNYMLNNYTKFQIAT-WGSLIVHEVLYFLFCLPGFLFQFI-----------   75
Mouse    31   EPFKNAWVYMLDNYTKFQIAT-WGSLIVHEAIYFLFSLPGFLFQFI-----------   75
Rat      31   EPFKNAWVYMLDNYTKFQIAT-WGSLIVHETIYFLFSLPGFLFQFI-----------   75
Yeast    28   NFMEKYWAAWYSYMNNDVLATGLMFFLLHEFMYFFRCLPWFIIDQI-----------   79

Human    76   ----------PYMKKYKIQ-------KDKPETWENQWKCFKVLLFNHPCIQLPLICGT  116
Chimp   116   PGEAGSETGTPGESSVSVAGSHLAAVQDKPETWENQWKCFKVLLFNHPCIQLPLICGT  173
Dog      76   ----------PFMKKYKIQ-------KDKPETWENQWKCFKVLLFNHFCIQLPLICGT  116
Mouse    76   ----------PYMRKYKIQ-------KDKPETFEGQWKCLKKILFNHFFIQLPLICGT  116
Rat      76   ----------PFMRKYKIQ-------KDKPETFEGQWKCLKGILFNHFFIQLPLICGT  116
Yeast    80   ----------PYFRRWKLQ-------PTKIPSAKEQLYCLKSVLLSHPLVEAIPIWTP  120

                                                  I          II    H173Q
human   117   YYFTEYFNIPYDWERMPRWYFLLARCFGCAVIEDTWHYFLHRLLHHKRIYKYIHKVHH  174
Chimp   174   YYFTEYFNIPYDWERMPRWYFLLARCFGCAVIEDTWHYFLHRLLHHKRIYKYIHKVHH  231
Dog     117   YYPTEYFNIPYDWERMPRWYMLLARCFGCAVIEDTWHYFLHRLLHHKRIYKYIHKVHH  174
Mouse   117   YYPTEFFNIPYDWERMPRWYLTLARCLGCAVIEDTWHYFLHRLLHHKRIYKYIHKVHH  174
Rat     117   YYFTEFFNIPYDWERMPRWYFTLARCLGCAVIEDTWHYFLHRLLHHKRIYKYIHKVHH  174
Yeast   121   HPMCEKLGITVEVP-FPSLKTMALEIGLFFVLEDTWHYMAHRLFHYGVFYKYIHKQHH  177
                                                  HXXXH      HXXHH

Human   175   EFQAPFGMEAEYAHPLETLILGTGFFIGIVLLCD-----HVILLWAWVTIRLLETIDV  227
Chimp   232   EFQAPFGMEAEYAHPLETLILGTGFFIGIVLLCD-----HVILLWAWVTIRLLETIDV  284
Dog     175   EFQAPFGMEAEYAHPLETLILGTGFFIGIMLLCD-----HVILLWAWVTIRLIETIDV  227
Mouse   175   EFQAPFGIEAEYAHPLETLILGTGFFIGIVLLCD-----HVILLWAWVTIRLLETIDV  227
Rat     175   EFQAPFGIEAEYAHPLETLILGTGFFIGIVLLCD-----HVILLWAWVTMRLLETIDV  227
Yeast   178   RYAAPFGLSAEYAHPAETLSLGPGTVGMPILYVMYTGKLHLFTLCVWITLRLPQAVDS  234

                  III          Y244C      IV
Human   228   HSGYDIPLNPLNLIPFYAGSRHHDFHHMNFIGNYASTFTWNDRIFGTDSQYNAYNEKR  285
Chimp   285   HSGYDIPLNPLNLIPFYAGSRHHDFHHMNFIGNYASTFTWNDRIFGTDSQYNAYNEKR  342
Dog     228   HSGYDIPLNPLNLIPFYAGSRHHDFHHMNFIGNYASTFTWNDRIFGTDSQFTAYNEKM  285
Mouse   229   HSGYDIPLNPLNLVPFYTGARHHDFHHMNFIGNYASTFTWNDKLFGTDAQYHAYIEKS  285
Rat     228   HSGYDIPLNPLNYIPFYTGARHHDFHHMNFIGNYASTFTWNDRIFGTDVQYHAYTEKM  285
Yeast   235   HSGYDFPWSLNKIMPFMAGAEHHDLHHHYFIGNYASSFRWNDYCLDTESGPEAKASRE  293
              HXXXH/D                  HXXEH

Human   286   KKPEKKTE--------  293
Chimp   343   KKPEKKTE--------  350
Dog     286   KKIEKKMQ--------  293
Mouse   286   KKLGKKSD--------  293
Rat     286   KKLGKKSE--------  293
Yeast   294   ERMKKRAENNAQKKTN  309
```

Figure 4. He et al., 2008